Remote Photoplethysmography: Evaluation of Contactless Heart Rate Measurement in an Information Systems Setting

Philipp V. Rouast [1], Marc T. P. Adam [2], Verena Dorner [1], Ewa Lux [1]

[1] Karlsruhe Institute of Technology, Germany
[2] The University of Newcastle, Australia

Abstract. As a source of valuable information about a person's affective state, heart rate data has the potential to improve both understanding and experience of human-computer interaction. Conventional methods for measuring heart rate use skin contact methods, where a measuring device must be worn by the user. In an Information Systems setting, a contactless approach without interference in the user's natural environment could prove to be advantageous. We develop an application that fulfils these conditions. The algorithm is based on remote photoplethysmography, taking advantage of the slight skin color variation that occurs periodically with the user's pulse. When evaluating this application in an Information Systems setting with various arousal levels and naturally moving subjects, we achieve an average root mean square error of 7.32 bpm for the best performing configuration. We find that a higher frame rate yields better results than a larger size of the moving measurement window. Regarding algorithm specifics, we find that a more detailed algorithm using the three RGB signals slightly outperforms a simple algorithm using only the green signal.

1 Introduction

Throughout the past decade, interest in affective states has been steadily increasing within Information Systems (IS) research [1]. Affective states provide valuable insights for the evaluation of artifacts in a number of IS related domains, with heart rate measurement (HRM) as one of the physiological measures typically employed for their assessment [2]. These domains include human-computer interaction and decision support systems. For instance, name please [3] used HRM to evaluate the impact of computerized agents on bidding behaviour in electronic auctions and name please [4] used neurophysiological correlates to investigate cognitive absorption in enactive training. There are many promising applications of real-time heart rate (HR) data as feedback signal in various IS domains, such as technostress applications [5], e-learning systems [6, 7], financial decision making [8–10], and electronic auctions [11–14].

Established methods for collecting HR data typically involve skin contact with electronic (electrocardiogram) or optical (photoplethysmogram) sensors. However, relatively new developments in affective computing make the need of skin contact for

HRM increasingly redundant. Subtle changes in the facial region can be captured remotely with RGB imaging, and an estimate of the HR derived. Due to their similarity to traditional photoplethysmography (PPG), such approaches are known as remote photoplethysmography (rPPG) [15]. The primarily used signal source in rPPG is a periodic color variation that occurs as light reflects off the skin and varies with blood volume [16]. While much earlier research on rPPG has demonstrated its feasibility in a stationary setting, more recent work focuses on settings where users are allowed to move naturally [15]. So far, very few studies had discussed online (i.e., real-time) applications of rPPG algorithms. We believe that real-time HRM could prove to be particularly useful for a range of applications in IS research, such as technostress applications, electronic commerce, and technology enhanced learning.

In this paper, we develop and evaluate a customizable approach for rPPG that is suitable for real-time applications. Our first research objective is to design an artifact with customizable parameters, based on existing approaches for rPPG, which enables both online and offline measurements and permits parameterization of the algorithm based on the computing capabilities of the platform [17]. We propose an algorithm based on the phenomenon of facial skin color variation to transform images from a video feed to HRM, in line with the general framework for rPPG proposed by [15]. In this way, unobtrusive HRM can be made available to researchers in various domains or directly integrated in systems as a real-time input. Our second research objective is to evaluate the artifact in an IS context, and use offline computations to study the impact of parameter variations on the feasibility of an online application. For this purpose, we conduct a lab experiment in which participants are asked to complete a series of arousal-inducing tasks.

The remainder of this paper is structured as follows: In Section 2, we discuss the theoretical foundation for the algorithm and review existing approaches for rPPG. Section 3 features a detailed description of our proposed algorithm, providing an overview of the configurable parameters of the algorithm. Details and results on the evaluation in an IS context are given in Section 4. We end with discussion and conclusion in Section 5.

2 Theoretical Background

In PPG, human HR is derived from an optically obtained volumetric measurement (plethysmogram) of the heart. Hertzman and Spealman [18] first noted that a variation in light transmission of a finger could be measured using a photoelectronic cell. This change in light transmission and reflection on the skin as an indication of cardiac activity is related to the optical properties of blood in motion [19]. Today, PPG using skin contact and dedicated light sources is also commonly used in smart watches and fitness bands, such as Fitbit Charge HR and Microsoft Band.

Only recently, researchers have started using ambient light sources and digital cameras to capture the plethysmographic signal remotely. Verkruysse et al. [20] showed that a video captured using an inexpensive, consumer-grade camera contained a rich enough plethysmographic signal to measure functions like HR and respiration rate.
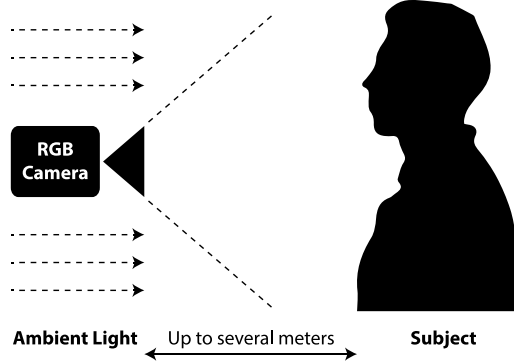
Fig. 1. A typical application of rPPG. An RGB camera captures at least the facial region of the subject which is illuminated by ambient light. The distance between camera and subject may be up to several meters

A typical application of rPPG (Figure 1) involves a subject – often seated at a desk – and a video camera positioned up to several meters away. The camera captures at least the subject's face, which is illuminated by ambient light. Any continuous segment of the resulting video sequence may be used to produce a HR estimate. If the temporal development of the HR is of interest, a sliding time window can be used to produce a series of HR estimates. Choosing the size of this sliding time window presents a trade-off: While a smaller time window reduces computational complexity and allows for a higher temporal resolution, a greater time window reduces the theoretically expected minimum estimation error. This estimation error follows from the frequency resolution $df = \frac{60}{T} bpm$, where T denotes the size of the sliding time window in seconds. For example, with a window size of 6 seconds, HR can only be measured with an accuracy of 10 bpm. Assuming uniformly distributed HR, it follows that the expected minimum estimation error equals $E[\varepsilon] = df/4$, or 2.5 bpm.

In the following, we discuss the three key steps in rPPG: (i) extraction of the raw signal, (ii) estimation of the plethysmographic signal, and (iii) HR estimation. There exists a multitude of possible choices for each of these three steps, choices being in part dependent on the specifics of the planned application. These include, e.g., expected movement of the subject and available resources for computation. In our case, we are specifically interested in an IS setting, i.e., users moving naturally while working at a desktop workstation.

2.1 Extraction of the Raw Signal

The first step in rPPG is extracting the raw signal from an input sequence of images of the subject's head. This generally involves a number of computations which are repeated and yield one or multiple real values for each input frame. A region of interest (ROI), usually in the subject's face, is marked in each frame. The raw signal is extracted as one or multiple of the RGB color channels using spatial pooling.

While in earlier work about rPPG the ROI was selected manually in the first frame of the video (e.g., [20, 21]), a common option nowadays is to use an algorithm for automated face detection to find facial boundaries [e.g., 19–21]. For more accurate position information, some researchers use algorithms for facial landmark detection [e.g., 22, 23] or skin detection [e.g., 21, 24].

The simplest choice for ROI is the bounding box returned by the classifier [e.g., 18, 25]. As this naïve ROI may cause noise due to included background pixels, many authors only include 60% of its width [e.g., 19, 20, 26]. Further research has shown that signal strength is not uniformly distributed over facial skin. The forehead and the cheeks exhibit maximum signal strength [30]. These areas are therefore common choices for ROI [e.g., 18, 28, 29].

Unless a subject remains absolutely stationary, the ROI needs to be updated for each frame in order to make the pixels in the ROI invariant to subject motion. In an IS setting with natural motion, this is an important component of the first step. Re-running the detection step for every frame [e.g., 19, 21, 30] is a simple, but not computationally efficient way to achieve this functionality. Some work [25, 31, 34] estimates an affine transformation for the ROI from frame to frame by tracking a set of suitable points in the face. This way, tracking arbitrary ROIs at reasonable levels of complexity becomes possible.

Finally, the raw signal is computed by spatially pooling all pixels comprising the chosen ROI [e.g., 17–19], i.e., averaging the values of the desired color channels within the ROI. While the green channel contains the strongest plethysmographic signal [20], both the red and blue channel also contain complementary information. Combinations of all three RGB channels [e.g., 19–21], two channels [21] as well as the green channel only [25, 26] have been used successfully.

2.2 Estimation of the Plethysmographic Signal

The raw signal can be interpreted as the temporal development of the absolute intensities of the selected RGB color channels. This multidimensional time series contains a periodic component, which corresponds to the HR, but also contains unwanted high- and low frequency noise. Low frequency noise can be caused by gradual movements and illumination changes; high frequency noise by sudden movements. The second step of rPPG aims at improving the signal-to-noise ration by removing frequencies that lie outside the frequency band expected for the HR. When multiple color channels are used, this step also reduces the signal to one dimension.

Since solely the periodicity of the signal is of interest, the raw signal is typically normalized before it is processed any further [e.g., 19, 20, 30]. Both unwanted high- and low frequency noise can be removed using a bandpass filter [e.g., 18, 22, 32]. Cut-off frequencies of 0.7 Hz and 4 Hz are usually applied [15]. Alternatively, low frequency noise can be removed by using a detrending filter [36] which presents a high pass equivalent. Correspondingly, high frequency noise can be removed with a low pass equivalent such as a moving average filter [e.g., 20, 22, 34].

If multiple channels are used, the dimensionality of the signal is typically reduced by linearly combining the channels. The optimal parameter choice for this combination is a much discussed issue. Most authors rely on techniques from the field of Blind

Source Separation (BSS) such as Independent Component Analysis (ICA) [e.g., 19, 20, 35] or Principal Component Analysis (PCA) [e.g., 18, 34, 36]. From the results, the component with the highest periodicity is selected, according to spectral power [e.g., 20, 21, 30].

2.3 HR Estimation

Given the estimated plethysmographic signal, the HR is estimated using frequency analysis. Most authors use an algorithm such as the Fast Fourier Transform (FFT) to perform a Discrete Fourier Transform (DFT) [e.g., 18, 19, 21]. Then, the index of the maximum power response in the frequency domain corresponds to the detected HR. If the individual beat-by-beat intervals are of interest, a peak detection algorithm should be applied [e.g., 20].

3 Approach

Between the choice of rPPG algorithm – e.g., signal used, steps to filter the signal and estimate the HR – and practical choices such as temporal window size and frame rate (due to limited computing resources, particularly in online analysis), there is a multitude of options for algorithm parametrization. We narrow the range of possible parameters down to three major choices, and evaluate their impact on the accuracy of HR estimation in the following section.

Table 1. Command line arguments for the rPPG application. Each argument has several options and a default parameter setting.

Flag	Description	Options
-i	Path to input video	Omit flag to use webcam
-a	Specify rPPG algorithm variant	*g* to use only green channel (default)
		rgb to use red, green, and blue channel with PCA
-max	Maximum size of the sliding time window in seconds	Any positive integer (default: *6*)
-ds	Down-sample by using every xth frame	Any positive integer (default: *1*)
-gui	Display the GUI	*true* or *false* (default: *true*)
-r	Re-detection interval in seconds	Any positive integer (default: *1*)

We developed a command line rPPG application that takes as input either a video file or a real-time feed from a video camera. The application supports a simple rPPG algorithm that uses only the green channel, and a more advanced rPPG algorithm that uses all RGB channels. Both algorithms use filtering methods commonly used in past works on rPPG. HR estimates are calculated and written to a log file for every step using a

sliding window with customizable size. If a video is used as input, the frame rate can optionally be downsampled. Table 1 lists the available parameters.

Both pre-recorded input video and real-time webcam feed are handled by the same algorithm. For pre-recorded input, the effectively achieved frame rate is pre-determined, but can be downsampled. For real-time video, the achieved frame rate is dynamic and dependent on the computation rate. Once a face is recognized, the time window is populated with raw data and estimates are produced once the minimum window size is reached. The window starts moving when the maximum size is reached, such that new estimates are always based on the past seconds in the window. If the GUI is activated, this process is visualized.

We use the Viola-Jones (VJ) object detector [40] as most previous works do [15] to find the biggest face in the frame. Using Haar-like features, this classifier is trained to detect frontal faces and returns a bounding box of the detected object. Once a face has been detected, we use the coordinates of the bounding box to select a rectangle on the forehead as the ROI. Specifically, the ROI has 40% of bounding box width and 15% of bounding box height, as shown graphically in Fig. 2. Both the bounding box and ROI are tracked in subsequent frames. For this, we find a set of prominent tracking points within the ROI selected using the algorithm of [41]. These points are subsequently tracked from frame to frame using the Kanade-Lucas-Tomasi algorithm [42]. We then use the two sets of original and tracked points to calculate an optimal affine transform which is applied to the bounding box of the face and ROI, similar to the approach of [31]. Thus, we are able to track the ROI smoothly without having to run face detection for every frame. For greater robustness, we re-detect the face at an adjustable interval.
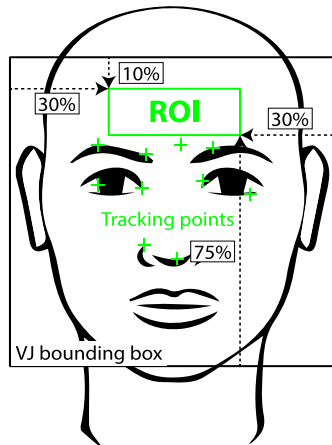

Fig. 2. The ROI is defined based on the bounding box from the Viola-Jones algorithm. A set of tracking points is used to update the ROI in subsequent frames

By applying the respective ROI as a mask, we extract the raw signal as the average R, G, and B channels for every frame. This step gives the one-dimensional green signal for the simple algorithm variant and the three-dimensional RGB signal for the more advanced rPPG algorithm. Depending on the effective frame rate and window size, the length of the signal can vary, e.g., from 90 frames (at a window size of 6 seconds and

effective frame rate of 15 frames per second (fps)) to 360 frames (at a window size of 12 seconds and effective frame rate of 30 fps).

The rPPG application then removes unwanted high- and low frequency noise. Since re-detection can cause the ROI to 'jump', which is reflected in the raw signal, we initially apply a custom filter to clear any rapid leaps caused by re-detection. To this end, we keep track of when re-detection occurred and set the first difference in the signal to zero in these instances. In the following steps, we have chosen common choices from existing work on rPPG [15]. The resulting de-noised signal is first normalized, the level being irrelevant for our analysis. Low frequency noise, typically a trend in the signal, is subsequently removed with the advanced detrending filter proposed by [36]. Finally, we remove high frequency noise by applying a moving average filter to the signal. Fig. 3 illustrates these steps using exemplary data from the green channel.
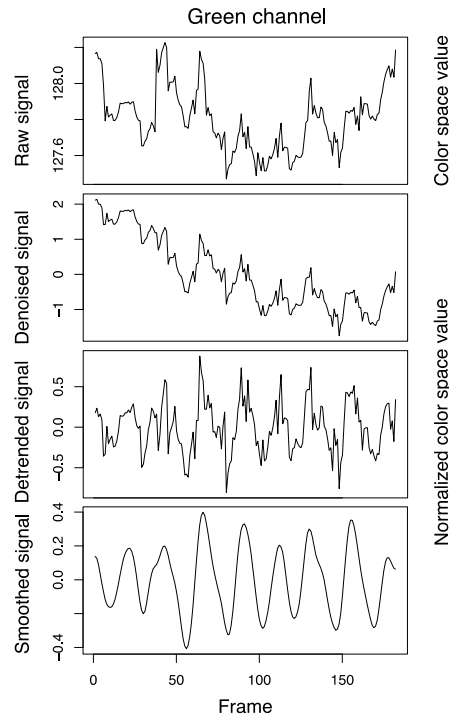

Fig. 3. Exemplary values for a simple rPPG algorithm using only the green channel

In the case of the simple rPPG algorithm variant, the steps described above are applied to the one-dimensional signal from the green channel as in Fig. 3, to yield the estimated plethysmographic signal with a distinct periodicity. For the advanced approach using the RGB channels, the first three steps are applied to each channel individually: Removal of noise due to re-detection, normalization and detrending. Hereafter, we run a PCA using the three filtered RGB channels. The PCA produces three linearly uncorrelated components, each a linear combination of the three RGB signals. Following [21], we assume that one of the components corresponds to the plethysmographic signal,

containing a distinct periodicity. We hence select the component with the most distinct periodicity: After converting each component to the frequency domain using a DFT, we find the maximum power response of a single frequency for each component. The component with the greatest power response is selected. Finally, we apply a moving average filter to this component to remove the remaining high frequency noise, yielding the estimated plethysmographic signal for this algorithm. Fig. 4 reports exemplary data for this approach using the same video as Fig. 3. Note that the selected principal component in this example is very similar to the filtered signal from the green channel.
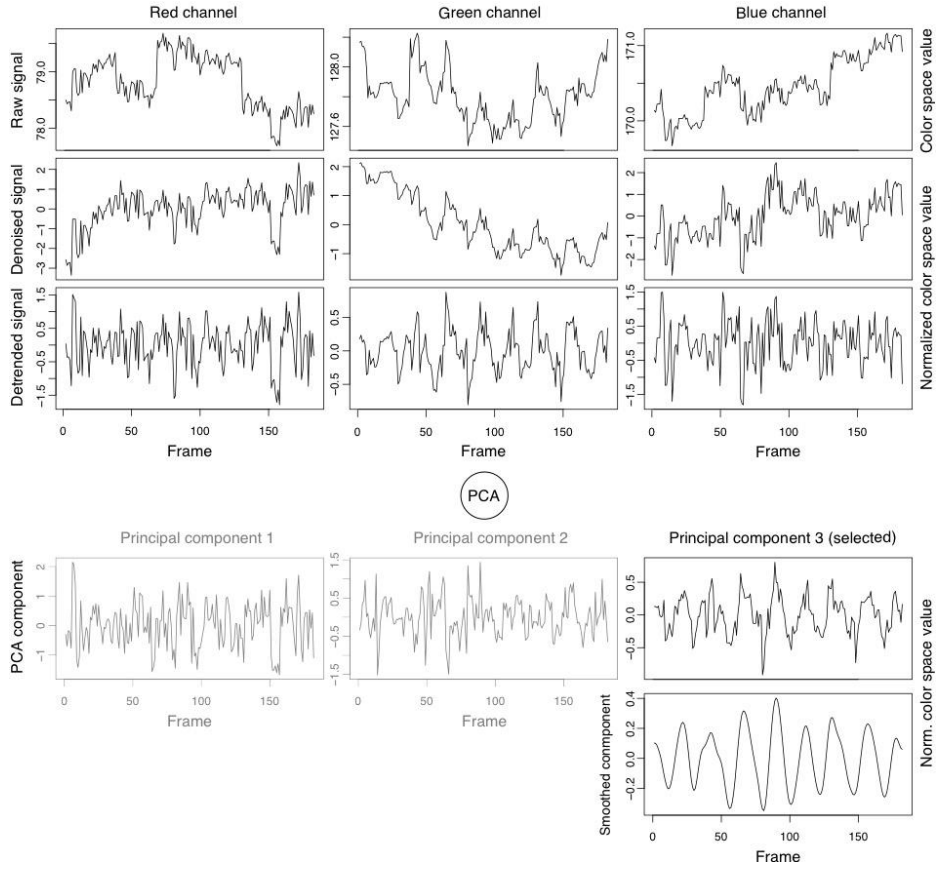

Fig. 4. Exemplary values for an rPPG algorithm using all three RGB channels. The PCA is used to produce three components, from which the one with the highest periodicity is selected

Estimation of the HR concludes each rPPG algorithm. Using the DFT, the plethysmographic signal is converted to the frequency domain, and we find the frequency with the maximum power response. Using the frequency index of the maximum power response i, the size of the signal N, and the effective sampling rate f_s, we calculate the corresponding HR estimate as $\widehat{HR} = \frac{i}{N} f_s$.

4. Experimental Evaluation

Data for the evaluation of both rPPG algorithm variants was collected in a lab experiment at KD2Lab in Karlsruhe, Germany.[1] A total of 20 participants (8 females, 12 males) were recruited from a pool of students. Each participant was seated at a desk in front of a computer monitor and asked to participate in four different experiment phases with differing tasks. Meanwhile, the participant was recorded on video using a Logitech C270 webcam at 640x480 VGA resolution and a frame rate of 30 fps. The video was encoded using the H.264 codec and stored in an mp4 container. Distance from the camera was approximately 0.5 m. Baseline HR data was collected simultaneously using Bioplux finger PPG and Bioplux ECG [43]. During the experiment, participants moved naturally when interacting with the computer and working on the experiment tasks. All participants gave consent to having their video and physiological data used for HR estimation and validation.
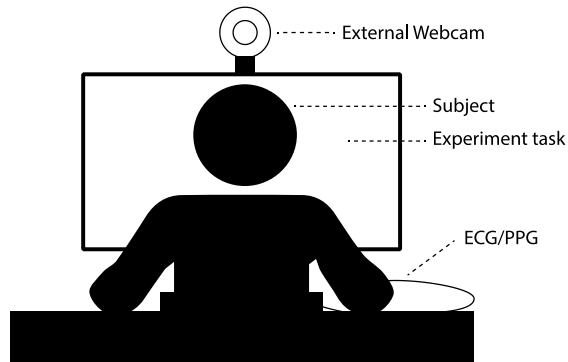

Fig. 5. Experimental setup: The subject is seated at a desk and presented with an experiment task. Video and HR data are captured using webcam and ECG/PPG

The experiment comprised four phases which differed with regard to levels of arousal and mobility. Before each experiment phase, the participant received written instructions on paper, such that he/she had the opportunity to read them while they were played back from an audio recording. Instructions also included information about the performance-based payoff in real money. After each phase, the participant filled out a short questionnaire on-screen.

The first phase was a rest phase, where participants were asked to relax for five minutes. This was followed by two phases with dynamic auctions. We built on the design of a recent Dutch auction experiment by [44], since this dynamic auction format is known to induce emotional arousal. In order to induce different levels of emotional arousal, one block of six auctions was configured with low value uncertainty and low time pressure (clock speed: 0.4 seconds per price step), the other block of six auctions with high value uncertainty and high time pressure (clock speed: 0.2 seconds per price step). The order of these two phases was varied randomly and duration was approximately 5 and 8 minutes for the fast and slow Dutch auctions, respectively. The fourth

---

[1] A computer-based experimental laboratory, see http://www.kd2lab.kit.edu/.

and last phase consisted of an arousal inducing task as described in [45]. Here, participants were asked to find a specific sequence of symbols amongst 20 alternatives under time pressure. This last phase took 5 minutes. Including instructions, questionnaires and test rounds, experiment duration averaged approximately 32 minutes. The experimental software was implemented in Brownie [46, 47].

5. Results

Our evaluation focuses on the effect on HRM accuracy of (i) the selection of color channels, (ii) the frame rate, and (iii) the size of the time windows. First, with respect to *selection of color channels*, we apply one parametrization where only the green channel (henceforth the *G* algorithm) is used. In a further parametrization, all three RGB channels are combined using a PCA (henceforth the *RGB* algorithm). All other steps (apart from signal choice and additional use of the PCA) are identical. Second, with respect to the impact of the effective *frame rate* on HR accuracy, we compare the results achieved using video at 30 fps to the results achieved using down-sampled video at 15 fps. Third, with respect to *size of the time window*, we investigate the difference in accuracy at window sizes of 6 seconds and 12 seconds. Theoretically, a larger window decreases the expected minimum estimation error as discussed in Section 2, but possible side-effects on typical errors in rPPG are unclear.

Table 2. Average RMSE for different algorithm and parameter combinations

Algorithm		G		RGB	
		window size		window size	
		6 seconds	12 seconds	6 seconds	12 seconds
frame	15 fps	$\overline{RMSE}$	$\overline{RMSE}$	$\overline{RMSE}$	$\overline{RMSE}$
		12.26 bpm	13.70 bpm	10.53 bpm	11.20 bpm
rate	30 fps	$\overline{RMSE}$	$\overline{RMSE}$	$\overline{RMSE}$	$\overline{RMSE}$
		8.72 bpm	9.12 bpm	8.18 bpm	7.32 bpm

To reiterate, we are interested in detecting the temporal development of HR using rPPG. We calculated HR as mean HR based on rPPG every 10 seconds and, for validation, mean HR based on the finger clip PPG sensor. Missing data for this baseline measurement was complemented using the ECG measurements. For each participant and experiment phase, this gives us the root mean square error (RMSE) between a given rPPG configuration and the baseline HRM. Our analysis is based on all four phases of the experiment. Table 2 lists the mean RMSE for the different algorithm and parameter combinations. For each algorithm-parameter combination, this represents the mean RMSE across all participants and phases.

In the following, we discuss the implication of these results with regards to the choice of algorithm, frame rate, and window size. A visualization of the results including error bars is displayed in Fig. 6.
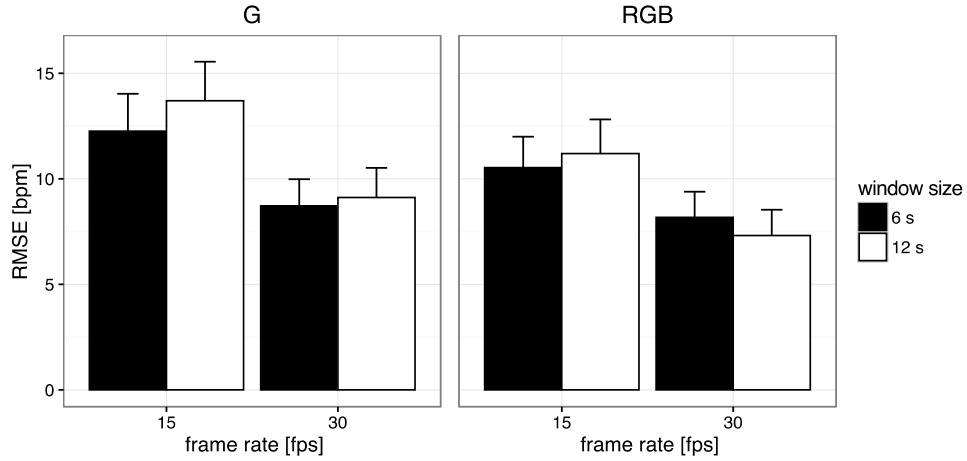
Fig. 6. Average RMSE for each algorithm and parameter combination

An immediate observation from Fig. 6 is that the higher frame rate of 30 fps seems to lead to more accurate HRM across both algorithms and window sizes. This intuitive finding is supported by Welch t-tests: The null hypothesis of error rates being equal can be rejected for each combination of algorithm and window size (algorithm G and window size 6s: p = .0015; G and 12s: p = .0001; RGB and 6s: p = .015; RGB and 12s: p = .0002). In contrast, the window size used in our rPPG algorithms does not have a significant effect on the average RMSE, despite the theoretically smaller minimum estimation error. Due to the higher actual error rates, this effect may be irrelevant here. Note that on average, a greater window size leads to a higher RMSE for the G algorithm, although it is associated with a significantly higher computational complexity.

Table 3. Number of channels and frames for algorithm and parameter combination. The RGB algorithm uses three channels.

Algorithm		G		RGB	
		window size		window size	
		6 seconds	12 seconds	6 seconds	12 seconds
frame rate	15 fps	1 channel 90 frames	1 channel 180 frames	3 channels 90 frames	3 channels 190 frames
	30 fps	1 channel 180 frames	1 channel 360 frames	3 channels 180 frames	3 channels 360 frames

In general, the number of frames upon which HR estimation is based is a major determinant of the algorithm's computational complexity, which increases at least linearly with the number of frames. Both a combination of a 12 second window with a frame rate of 15 fps and a 6 second window with a frame rate of 30 fps lead to 180 frames in the buffer per channel (Table 3), such that the respective increase in computational complexity is comparable. Hence, our results indicate that for both implemented algorithms, a higher frame rate should be preferred over a larger window size.

Comparing the two rPPG algorithm variants, the RGB version *on average* performs better for all combinations of frame rate and window size. Using Welch *t*-tests, a significant difference can be detected for the combination with window size of 12 seconds (For frame rate 15fps: p = .0444; for 30fps: p = .0559). Hence, considering the additional computational complexity of two channels and PCA, we recommend choosing the G approach for scenarios where computation power is costly, such as an online application scenario, particularly in mobile settings, and the RGB approach when computation with a larger window size can be done offline.

Since we are particularly interested in online non-stationary settings, we now have a closer look at the G algorithm with a window of 6 seconds and the RGB algorithm with a window of 12 seconds. For each, we choose the full frame rate of 30 seconds. Fig. 7 gives an example for a participant where rPPG using the RGB algorithm performed comparably well, with RMSE between 5 and 7 bpm. The experiment phases (rest phase, two auction phases and arousal task) are marked in grey.
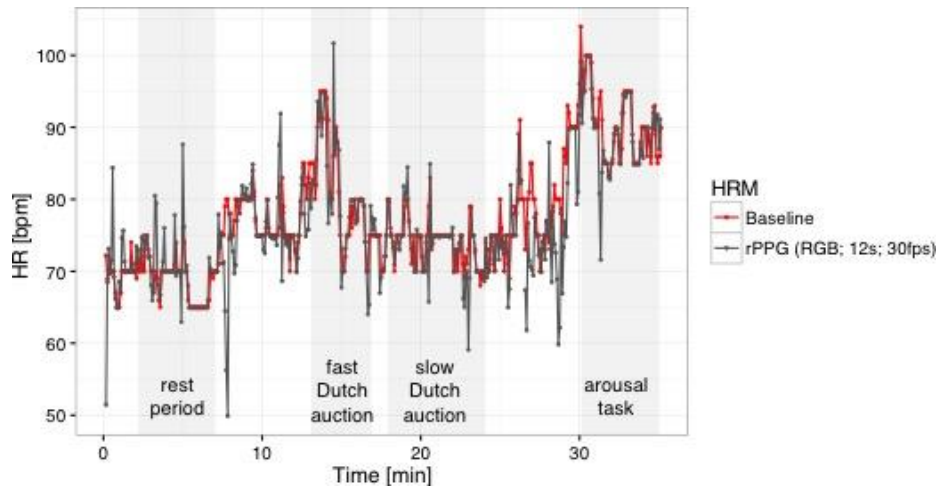

Fig. 7. Timeline of a participant's HR Baseline measurement and corresponding rPPG measurements. Experiment phases are marked in grey

In the first auction phase and the arousal game, the participant's HR peaks when the task starts and then decreases. This temporal development of the participant's affective state is captured by the rPPG algorithm. In between phases, and occasionally within phases, outliers are observable that could be removed in a more sophisticated rPPG algorithm, e.g., by removing values that are outside a certain range. Note that participants were reading instructions in between phases, possible turning their face away from the camera, which may explain some of the inaccuracies between phases.

In a direct comparison between the selected G and RGB algorithms, the difference in accuracy can be compared beyond the average RMSE found in Table 3. Using all individual pairs of HRM from rPPG and Bioplux baseline, we find a correlation of Pearson's *r* = .64 for the G algorithm, and Pearson's *r* = .73 for the RGB algorithm. This difference is visualized in Fig. 8. Note that due to the large amount of data points,

outliers appear visually slightly exaggerated. Points are colored according to the experiment phase they were recorded in.
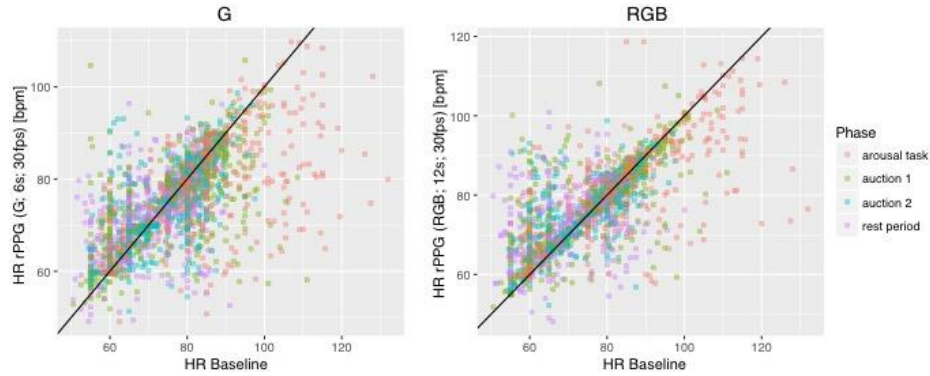

Fig. 8. Scatterplot of Baseline versus rPPG HRM for two selected algorithms

For both algorithms, many of the extreme outliers appear to belong to the phase of the arousal task, which may be attributed to both the higher HR and increased subject movement in this phase. There does not appear to be any significant measurement bias for the algorithms: On average, the G algorithm underestimates the baseline HR by 1.01 bpm, while the RGB algorithm overestimates the baseline by .85 bpm.

6. Conclusion and Outlook

In an IS context, HR data are becoming increasingly valuable as a source of information about a subject's affective states [3, 4, 48]. The recently explored methods for remote HRM using rPPG [15] promise a low-cost application without interfering in a professional work environment, enabling less obtrusive measurements in situ.

In this paper, we introduced a customizable implementation of rPPG with low-cost RGB cameras. This implementation is based on an approach representative for existing work on rPPG and draws on methods commonly used to measure the HR based on rPPG. Customizing options include (i) choice of using the green channel only or all available RGB channels, (ii) sampling rate, and (iii) window size used for measurements. As computational resources are limited in online environments and particularly when using mobile devices, we evaluated different parametrizations of our rPPG implementation in a laboratory experiment with 20 participants who participated in four tasks to induce different levels of emotional arousal.

We find that the frame rate has a significant influence on HRM accuracy. Higher frame rates, rather than larger window sizes, improve HRM accuracy considerably. Concerning the choice of signal channels, we find that using all three RGB channels delivers slightly better results on average, especially in combination with a larger measurement window. If computational resources are sparse however, we recommend falling back to the green channel, which carries the strongest plethysmographic signal.

While the overall RMSE is not as small as reported in other work on rPPG [15], it is known that error rates are difficult to compare, since they depend on a number of circumstances, such as the movements patterns due to the experimental task or laboratory setting. Our application concentrates on the temporal development of HR as we consider a continuous series of measurements made using rPPG in tasks with different levels of arousal. We developed an application for rPPG measurements that can be used for video file or real-time feeds from a video camera and provide a set of parameters that can be adjusted to increase measurement accuracy. Hence, our work is encouraging for future work on real-time applications of rPPG.

References

1. Riedl, R., Davis, F.D., Hevner, A.R.: Towards a NeuroIS Research Methodology: Intensifying the Discussion on Methods, Tools, and Measurement. J. Assoc. Inf. Syst. 15 (2014) i–xxxv
2. Adam, M.T.P., Krämer, J., Gamer, M., Weinhardt, C.: Measuring emotions in electronic markets. In: ICIS 2011 Proceedings. (2011) 1–19
3. Teubner, T., Adam, M.T.P., Riordan, R.: The Impact of Computerized Agents on Immediate Emotions, Overall Arousal and Bidding Behavior in Electronic Auctions. J. Assoc. Inf. Syst. 16 (2015) 838–879
4. Léger, P.-M., Davis, F.D., Cronan, T.P., Perret, J.: Neurophysiological Correlates of Cognitive Absorption in an Enactive Training Context. Comput. Human Behav. 34 (2014) 273–283
5. Adam, M.T.P., Gimpel, H., Maedche, A., Riedl, R.: Design Blueprint for Stress-sensitive Adaptive Enterprise Systems. Bus. Inf. Syst. Eng. (2016)
6. Shen, L., Wang, M., Shen, R.: Affective E-Learning: Using "Emotional" Data to Improve Learning in Pervasive Learning Environment. Educ. Technol. Soc. 12 (2009) 176–189
7. Astor, P.J., Adam, M.T.P., Jerčić, P., Schaaff, K., Weinhardt, C.: Integrating biosignals into information systems: A neurois tool for improving emotion regulation. J. Manag. Inf. Syst. 30 (2013) 247–278
8. Hariharan, A., Adam, M.T.P.: Blended Emotion Detection For Decision Support. IEEE Trans. Human-Machine Syst. 45 (2015) 510–517
9. Adam, M.T.P., Kroll, E.B.: Physiological evidence of attraction to chance. J. Neurosci. Psychol. Econ. 5 (2012) 152–165
10. Hariharan, A., Adam, M.T.P., Astor, P.J., Weinhardt, C.: Emotion regulation and behavior in an individual decision trading experiment: Insights from psychophysiology. J. Neurosci. Psychol. Econ. 8 (2015) 186–202
11. Adam, M.T.P., Krämer, J., Müller, M.B.: Auction fever! How time pressure and social competition affect bidders' arousal and bids in retail auctions. J. Retail. 91 (2015) 468–485
12. Adam, M.T.P., Krämer, J., Weinhardt, C.: Excitement up! Price down! Measuring emotions in dutch auctions. Int. J. Electron. Commer. 13 (2012) 7–39
13. Adam, M.T.P., Astor, P.J., Krämer, J.: Affective images, emotion regulation

and bidding behavior: An experiment on the influence of competition and community emotions in internet auctions. J. Interact. Mark. 35 (2016) 56–69

14. Müller, M.B., Adam, M.T.P., Cornforth, D.J., Chiong, R., Krämer, J., Weinhardt, C.: Selecting physiological features for predicting bidding behavior in electronic auctions. In: Proceedings of the Forty-Ninth Annual Hawaii International Conference on System Sciences (HICSS). (2016) 396–405

15. Rouast, P. V, Adam, M.T.P., Chiong, R., Cornforth, D.J., Lux, E.: Remote heart rate measurement using low-cost RGB face video: A technical literature review. Front. Comput. Sci. (2016)

16. Allen, J.: Photoplethysmography and its application in clinical physiological measurement. Physiol. Meas. 28 (2007) R1–R39

17. Rouast, P. V, Adam, M.T.P., Cornforth, D.J., Lux, E., Weinhardt, C.: Using contactless heart rate measurements for real-time assessment of affective states. In: Davis, F.D., Riedl, R., Vom Brocke, J., Léger, P.-M., and Randolph, A.B. (eds.): Information Systems and Neuroscience. (2016)

18. Hertzman, A.B., Spealman, C.R.: Observations on the finger volume pulse recorded photoelectrically. Am. J. Physiol. 119 (1937) 334–335

19. Roberts, V.C.: Photoplethysmography - fundamental aspects of the optical properties of blood in motion. Trans. Inst. Meas. Control. 4 (1982) 101–106

20. Verkruysse, W., Svaasand, L.O., Nelson, J.S.: Remote plethysmographic imaging using ambient light. Opt. Express. 16 (2008) 21434–21445

21. Lewandowska, M., Ruminski, J., Kocejko, T.: Measuring pulse rate with a webcam - A non-contact method for evaluating cardiac activity. In: Proceedings of the 2011 Federated Conference on Computer Science and Information Systems (FedCSIS). (2011) 405–410

22. Poh, M.-Z., McDuff, D.J., Picard, R.W.: Non-contact, automated cardiac pulse measurements using video imaging and blind source separation. Opt. Express. 18 (2010) 10762–10774

23. Poh, M.-Z., McDuff, D.J., Picard, R.W.: Advancements in noncontact, multiparameter physiological measurements using a webcam. IEEE Trans. Biomed. Eng. 58 (2011) 7–11

24. De Haan, G., Jeanne, V.: Robust pulse rate from chrominance-based rPPG. IEEE Trans. Biomed. Eng. 60 (2013) 2878–2886

25. Li, X., Chen, J., Zhao, G., Pietikäinen, M.: Remote heart rate measurement from face videos under realistic situations. In: Proceedings of the 2014 IEEE Computer Society Conference on Computer Vision and Pattern Recognition. (2014) 4264–4271

26. Tasli, H.E., Gudi, A., Den Uyl, M.: Remote ppg based vital sign measurement using adaptive facial regions. In: Proceedings of the 2014 IEEE International Conference on Image Processing (ICIP). (2014) 1410–1414

27. Lee, K.-Z., Hung, P.-C., Tsai, L.-W.: Contact-free heart rate measurement using a camera. In: Proceedings of the 2012 Ninth Conference on Computer and Robot Vision (CRV). (2012) 147–152

28. Xu, S., Sun, L., Rohde, G.K.: Robust efficient estimation of heart rate pulse from video. Biomed. Opt. Express. 5 (2014) 1124–35

29. Wei, L., Tian, Y., Wang, Y., Ebrahimi, T.: Automatic webcam-based human heart rate measurements using laplacian eigenmap. In: Lecture Notes in

Computer Science. (2013) 281–292

30. Lempe, G., Zaunseder, S., Wirthgen, T., Zipser, S., Malberg, H.: Roi selection for remote photoplethysmography. In: Meinzer, H.-P., Deserno, M.T., Handels, H., and Tolxdorff, T. (eds.): Informatik aktuell. (2013) 99–103

31. Feng, L., Po, L.-M., Xu, X., Li, Y.: Motion artifacts suppression for remote imaging photoplethysmography. In: Proceedings of the 19th International Conference on Digital Signal Processing (DSP). (2014) 18–23

32. Feng, L., Po, L.M., Xu, X., Li, Y., Ma, R.: Motion-resistant remote imaging photoplethysmography based on the optical properties of skin. IEEE Trans. Circuits Syst. Video Technol. 25 (2015) 879–891

33. Kwon, S., Kim, H., Park, K.S.: Validation of heart rate extraction using video imaging on a built-in camera system of a smartphone. In: Proceedings of the 2012 IEEE Annual International Conference of the Engineering in Medicine and Biology Society. (2012) 2174–2177

34. Kumar, M., Veeraraghavan, A., Sabharwal, A.: DistancePPG: Robust non-contact vital signs monitoring using a camera. Biomed. Opt. Express. 6 (2015) 1565–1588

35. Hsu, Y., Lin, Y.L., Hsu, W.: Learning-based heart rate detection from remote photoplethysmography features. In: Proceedings of the 2014 IEEE International Conference on Acoustics, Speech and Signal Processing (ICASSP). (2014) 4433–4437

36. Tarvainen, M.P., Ranta-Aho, P.O., Karjalainen, P.A.: An advanced detrending method with application to hrv analysis. IEEE Trans. Biomed. Eng. 49 (2002) 172–175

37. Holton, B.D., Mannapperuma, K., Lesniewski, P.J., Thomas, J.C.: Signal recovery in imaging photoplethysmography. Physiol. Meas. 34 (2013) 1499–1511

38. McDuff, D., Gontarek, S., Picard, R.W.: Improvements in remote cardiopulmonary measurement using a five band digital camera. IEEE Trans. Biomed. Eng. 61 (2014) 2593–2601

39. Wang, W., Stuijk, S., De Haan, G.: Exploiting spatial redundancy of image sensor for motion robust rppg. IEEE Trans. Biomed. Eng. 62 (2015) 415–425

40. Viola, P., Jones, M.: Rapid object detection using a boosted cascade of simple features. In: Proceedings of the 2001 IEEE Computer Society Conference on Computer Vision and Pattern Recognition. (2001) 511–518

41. Shi, J., Tomasi, C.: Good features to track. In: Proceedings of the 1994 IEEE Computer Society Conference on Computer Vision and Pattern Recognition. (1994) 593–600

42. Lucas, B.D., Kanade, T.: An iterative image registration technique with an application to stereo vision. In: Proceedings of the 7th International Joint Conference on Artificial Intelligence (IJCAI). (1981) 674–679

43. Bioplux: Wireless Biosognals, http://www.plux.info/index.php/en/ [accessed 2016-08-19]

44. Hariharan, A., Adam, M.T.P., Teubner, T., Weinhardt, C.: Think, feel, bid: The impact of environmental conditions on the role of bidders' cognitive and affective processes in auction bidding. Electron. Mark. (2016) 1–17

45. Schaaff, K., Degen, R., Adler, N., Adam, M.T.P.: Measuring Affect Using a

Standard Mouse Device. Biomed. Eng. (NY). 57 (2012) 761–764

46. Hariharan, A., Adam, M.T.P., Dorner, V., Lux, E., Müller, M.B., Pfeiffer, J., Weinhardt, C.: Brownie: A platform for conducting neurois experiments. (2015)

47. Müller, M.B., Hariharan, A., Adam, M.T.P.: A NeuroIS Platform for Lab Experiments. In: Gmunden Retreat on NeuroIS. (2014) 15–17

48. Riedl, R.: On the biology of technostress: Literature review and research agenda. ACM SIGMIS Database. 44 (2013) 18–55